Article

Not peer-reviewed version

Low Molecular Weight Inhibitors Targeting the RNA-Binding Protein HuR

Benjamin Philipp Joseph , Verena Weber , Lisa Knüpfer , Alejandro Giorgetti , Mercedes Alfonso-Prieto , Sybille Krauß * , Paolo Carloni * , Giulia Rossetti *

Posted Date: 3 August 2023

doi: 10.20944/preprints202308.0290.v1

Keywords: RNA-binding protein; human antigen R (HuR); high-throughput virtual screening; small molecule inhibitors; RNA pulldown assay

Article

Low Molezcular Weight Inhibitors Targeting the RNA-Binding Protein HuR

Benjamin Philipp Joseph [1,2,†], Verena Weber [1,2,†], Lisa Knüpfer [3], Alejandro Giorgetti [1,4], Mercedes Alfonso-Prieto [1], Sybille Krauß [3,*], Paolo Carloni [1,2,*] and Giulia Rossetti [1,5,6,*]

[1] Institute for Neuroscience and Medicine and Institute for Advanced Simulations (INM-9/IAS-5), Computational Biomedicine, Forschungszentrum Jülich, 52425 Jülich, Germany
[2] Faculty of Mathematics, Computer Science and Natural Sciences, RWTH Aachen, 52062 Aachen, Germany
[3] Institute of Biology, University of Siegen, 57076 Siegen, Germany
[4] Department of Biotechnology, University of Verona, 37134 Verona, Italy
[5] Jülich Supercomputing Centre (JSC), Forschungszentrum Jülich, 52425 Jülich, Germany
[6] Department of Neurology, RWTH Aachen University, 44517 Aachen, Germany
* Correspondence: sybille.krauss@uni-siegen.de (S.K.); p.carloni@fz-juelich.de (P.C.); g.rossetti@fz-juelich.de (G.R.)
† Shared first authorship.

Abstract: The RNA-binding protein Human antigen R (HuR) regulates stability, translation, and nucleus-to-cytoplasm shuttling of its target mRNAs. The protein has been progressively recognized as a relevant therapeutic target for several pathologies like cancer, neurodegeneration, as well as inflammation. Inhibitors of mRNA binding to HuR might thus be beneficial against a variety of diseases. Here we present the rational identification of structurally novel HuR inhibitors. In particular, by combining chemoinformatics approaches, high throughput virtual screening and RNA–protein pull-down assays, we show that the 4-(2-(2,4,6-trioxotetrahydropyrimidin-5(2H)-ylidene)hydrazineyl)benzoate ligand exhibits dose-dependent HuR inhibition in binding experiments. Importantly, the chemical scaffold is new with respect to the so-far known HuR inhibitors, opening up a new avenue for the design of pharmaceutical agents targeting this important protein.

Keywords: RNA-binding protein; human antigen R (HuR); high-throughput virtual screening; small molecule inhibitors; RNA pulldown assay

1. Introduction

The Human antigen R (HuR) protein binds and stabilizes messenger RNA (mRNA) transcripts, enhancing their translation into proteins [1,2]. Therefore, it plays a critical role in post-transcriptional gene regulation [3], leading to a variety of processes, including cell proliferation [4], differentiation, stress response [5] and nociceptor function [6]. HuR dysregulation has been implicated in numerous diseases, including cancer [7–11], neurological disorders [12–16], and inflammatory diseases [17–19]. This makes HuR a very important target for pharmaceutical intervention.

Several therapeutic strategies have indeed been put forward [20–22], from RNA interference [23,24] and immunotherapy [25] to natural compounds [26,27] and small molecule inhibitors [27–29]. The latter impair either mRNA binding or HuR translocation to the cytoplasm. RNA interference and immunotherapy are still in their early stages for HuR, with several limitations [30]. The use of natural compounds can pose challenges like variable potency and specificity or limited bioavailability [31]. Instead, therapeutic strategies based on small molecules are very promising. Examples of *in vitro* and *in cellulo* validated ligands (including some low weight natural products) are: sulfonyl aromatics [28], coumarins [27] and flavonoids [26] (see Table S1). A few successful small molecules that were experimentally proven to bind HuR proteins *in vivo* include embelin [32], okicenone [29], triptolide [33], leptomycin B [34], selinexor [35], KH-3 and derivatives [36], suramin [37], mitoxantrone [38],

Preprints (www.preprints.org) | NOT PEER-REVIEWED | Posted: 3 August 2023 doi:10.20944/preprints202308.0290.v1

and DHTS [39] (see Figure S1). One *in vivo* tested ligand, MS-444 [40], is currently in preclinical studies [41].

Structural insights on HuR in the free state and in complex with *in vivo* ligands have been provided by X-ray crystallography, NMR and fluorescence polarization assays. The HuR protein contains three RNA recognition motifs (RRM1-3) (Figure 1), responsible for binding adenylate and uridylate (AU)-rich elements (AREs) [2,42] in mRNA, through highly conserved ribonucleoprotein (RNP) sequences [43]. RRM1 and RRM2 are separated by a short, 10 amino acid linker, whereas a longer, ~50 residue hinge region connects the third RRM3 motif (see Figure 1). This hinge bears a nucleocytoplasmic shuttling element [44], that might transport HuR from the nucleus to the cytoplasm [44]. RRM1 initiates HuR's binding to AREs (K_D = 488 nM) [45]. Upon this first binding event, the RRM2 affinity for AREs increases (from K_D = 488 nM to K_D = 169 nM) [45]. Therefore RRM1-2 serves as the HuR anchoring point to the mRNA. The interdomain linker connecting RRM1/2 [24] and the charged surface of these two RRMs forms a cleft (of transient nature [45]) in the RNA-bound state (Figure 1B,C), with the target RNA fully occupying this cleft [45]. Ligands such as coumarins [27], DHTS [39] and KH-3 [36], as well as their derivatives, also bind to this transient cleft, though these small molecules can usually only partially fill the cleft [23,24]. This impairs the anchoring of RRM1-2 to the mRNA AREs, thus hampering mRNA recognition by HuR.

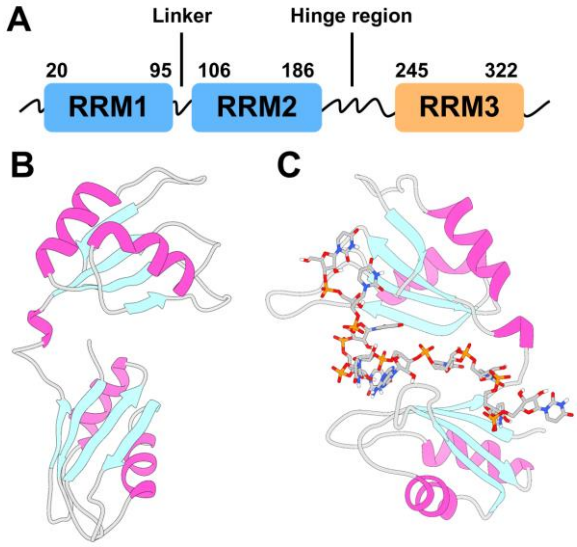

Figure 1. Human antigen R (HuR) protein topology and structure. (**A**) Scheme of the full-length HuR topology. HuR is composed of three highly conserved canonical RNA recognition motifs (RRMs). Each RRM domain adopts a βαββαβ topology, also called canonical αβ-sandwich, where a four-stranded antiparallel β-sheet is packed against two α-helices. (**B**,**C**) X-ray structures of HuR RRM1/2 alone (PDB code 4EGL [45]) and in complex with a 5'-AUUUUUAUUUU-3' target RNA (PDB code 4ED5 [45]). RRM2 and RRM1 correspond to the top and bottom domains, respectively.

RRM3 might stabilize the RRM1-2 complex [46] and, together with the hinge region, it might be important for interacting with other proteins [46], as well as for HuR dimerization [47] and multimerization in cancer cells [48]. *In vivo* tested ligands such as dehydromutactin [29], Okicenone [29], Triptolide [33], Leptomycin B [34], and Selinexor [35] have been suggested to bind to RRM3 (or the hinge region), thereby hindering HuR translocation to the cytoplasm [44].

Here, we have used computational methods to identify novel small molecules acting as HuR inhibitors, which were then successfully validated by experiments. Given the lack of 'enzymatic-like' binding cavities in RNA binding proteins such as HuR [49], we have exploited the aforementioned transient binding cleft between RRM1-2 to conduct a structure-based virtual screening combined with RNA pull-down assays. One promising compound emerged: 4-(2-(2,4,6-trioxotetrahydropyrimidin-5(2H)-ylidene)hydrazineyl)benzoate (STK018404 hereafter), already known as a potential antibacterial and antiviral (PubChem CID 942573). STK018404 not only has a

 doi:10.20944/preprints202308.0290.v1

very different chemical scaffold from the so far proposed inhibitors, but also shows a dose-dependent HuR inhibition in *in vitro* RNA binding experiments.

2. Results

2.1. Screening

We performed a structure-based virtual screening against the binding site previously identified by NMR for other small molecule HuR inhibitors [50], namely the above defined transient binding cleft between RRM1 and RRM2. The high-throughput virtual screening (HTVS) tool in Maestro from Schrödinger software [51,52] was used (see Methods for details), together with the following libraries: KIT (11,046 ligands), ENAMINE (200,057) and MOLPORT (8,084,644), for a total of approximately 8.3 million compounds. The screening resulted in 1,221 hits (Figure 2A), which were clustered according to the Butina algorithm [53], with Daylight fingerprints and Tanimoto similarity scores [54] and using a 0.3 cutoff (see Methods for further details). We then selected the 20 most populated clusters (Figure S2) and identified a representative molecule for each of them (Figure S3). Out of the 20 clusters, seven (clusters 3, 4, 10, 14, 17, 18 and 20) contain only compounds not available for purchase and thus could not be experimentally tested. Compounds belonging to the remaining thirteen clusters (Figure 2B) were selected for experimental testing based on their commercial availability. Specifically, the representatives of clusters 5, 11 and 19 were purchased directly. For clusters 7 and 9, a member of the respective cluster was bought. For clusters 1, 2, 6, 8, 12, 13, 15 and 16, a derivative structure of the cluster representative was purchased.

Preprints (www.preprints.org) | NOT PEER-REVIEWED | Posted: 3 August 2023 doi:10.20944/preprints202308.0290.v1

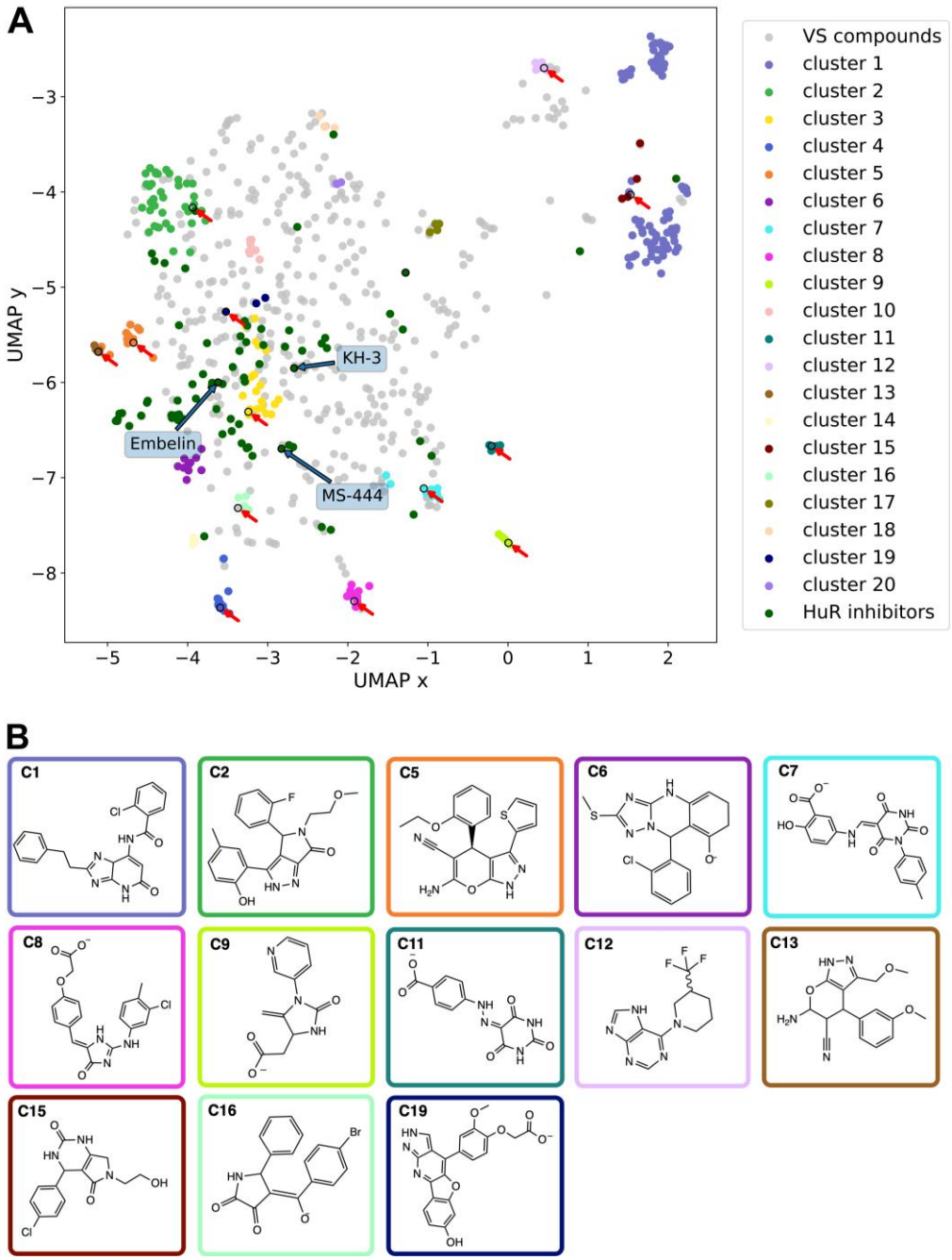

Figure 2. Chemical features of HuR ligands. (**A**) Representation of the chemical space occupied by the 1,221 hits identified here by virtual screening and 70 HuR inhibitors previously published as of January 2023 (see Table S1). Blue and red arrows indicate previously reported in vivo HuR inhibitors (see Figure S1) and hit molecules identified and tested experimentally in the present study, respectively. (**B**) Chemical structures of the compounds purchased for the thirteen HTVS clusters commercially available; the box colors indicate the corresponding clusters in (**A**). Representative, member and derivative indicate whether the compound corresponds to the cluster representative, a member of the cluster or a derivative compound. (C1) derivative, Z259632494; (C2) derivative, Z57908816; (C5) representative, 7643436; (C6) derivative, STK217448; (C7) member, STL170802; (C8) derivative, 5974204; (C9) member, Y044-6405; (C11) representative, STK018404; (C12) derivative, Z373002224; (C13) derivative, STK806137; (C15) derivative, STK593921; (C16) derivative, STL148963; (C19) representative, STL522523.

Preprints (www.preprints.org) | NOT PEER-REVIEWED | Posted: 3 August 2023 doi:10.20944/preprints202308.0290.v1

2.2. Comparison with the chemical space of the existing ligands

The chemical space of the HTVS identified hits was analyzed and compared with previously experimentally validated molecules targeting the RRM1-RRM2 binding cleft (hereafter called HuR inhibitors, see Table S1). To this aim, a nonlinear dimensionality-reduction technique, namely uniform manifold approximation and projection (UMAP) [55], was employed. As shown in Figure 2A, the molecules belonging to the 20 most populated clusters span a broader chemical space compared to the known inhibitors. Nonetheless, there is an overlap between the inhibitors and HTVS clusters 1, 2, 3 and 6, whereas clusters 7, 10, 14 and 16 are still in the vicinity of the inhibitors. In contrast, cluster groups 4, 8, 9, 11, 12, and 19 occupy distinct parts of the chemical space and consist of novel chemotypes when compared to previously reported HuR inhibitors (Figure 2A). This holds out the possibility to identify novel binding modes or chemical structures with a higher selectivity compared to the already available HuR inhibitors.

Mapping the protein-ligand interaction fingerprints (PLIFs) of each cluster group (stacked bar plot in Figures 3A and S4) shows no significant difference among the HTVS hits, despite their unique chemotypes. Comparing the PLIFs of the HTVS compounds (Figure 3A) with the previously reported inhibitors (Figure 3B), similar binding residues are identified. The key common residues are Ile23, Tyr63, Phe65, Arg97, Ile103 and Arg153, as they lie in the top six of the most contacted residues in both panels A and B. Interestingly, Ile23, Arg97, Ile103, Ile133 and Arg153 have been shown to participate in HuR binding to known inhibitors, as well as mRNA, by NMR and fluorescence polarization assays combined with mutagenesis [20,45,56].

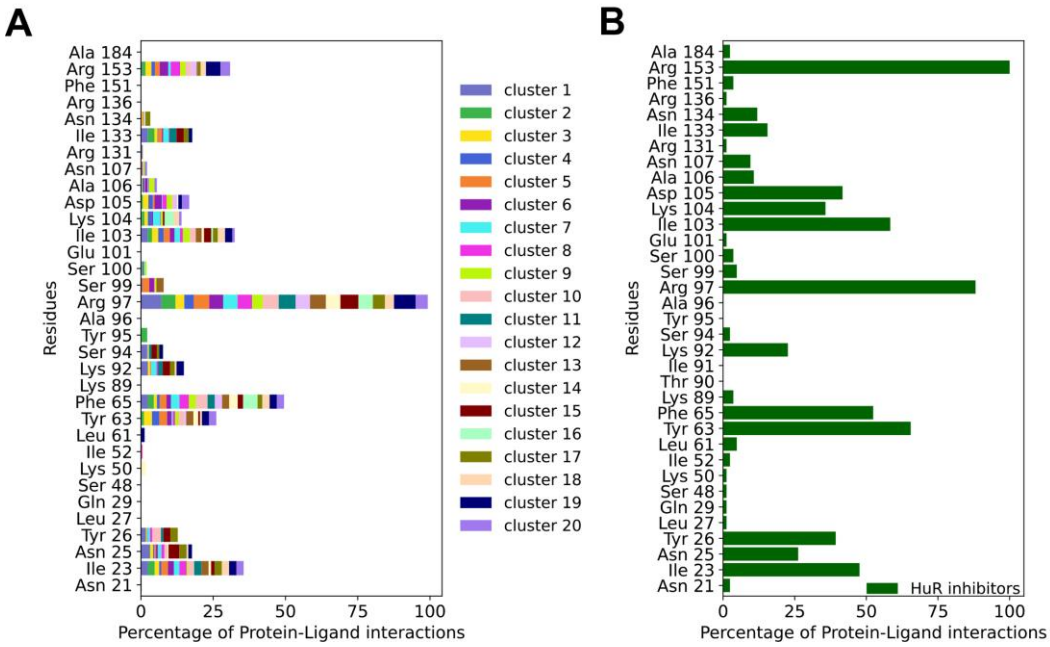

Figure 3. (**A**) Averages of the protein-ligand interaction fingerprints (PLIF) of the representative compounds of the HTVS clusters identified in this study vs (**B**) PLIF of previously reported HuR inhibitors. The normalization was done between the maximum and the minimum number of interactions for each PLIF. Specifically, in A PLIFs were normalized by the number of cluster members for each cluster and to the maximum number of interactions shared between all compounds (Arg 97), whereas in B PLIFs were normalized to the maximum number of interactions shared between all inhibitors (Arg 153).

For the HuR inhibitors, additional high contact frequency residues are Asn25, Tyr26, Lys92, Ser94, Lys104, Asp105, Ala106, Asn107 and Asn134. Two thirds of these residues were shown to form interactions with the RNA backbone (PDB 4ED5) [45], namely Asn25, Tyr26, Lys92, Lys104, Asn107 and Asn134. This is not unexpected, considering that HuR inhibitors aim at competing with mRNA binding.

Preprints (www.preprints.org) | NOT PEER-REVIEWED | Posted: 3 August 2023 doi:10.20944/preprints202308.0290.v1

2.3. Experimental test

As mentioned in the introduction, the HuR protein binds its target mRNAs through AU-rich elements. Thus, we used an AUUUUUAUUUU sequence (as in Figure 1B) to test if the predicted compounds affect the binding between the HuR protein and its target mRNA by performing RNA-protein pull-down assays. In particular, biotinylated RNA-oligos comprising the HuR-binding motif were incubated with cell extracts that contained the HuR protein in the presence or absence of the compounds. RNA-protein complexes were then purified with streptavidin-coated beads and RNA-bound proteins were analyzed by western blotting using an antibody detecting HuR. In addition, an experiment without RNA was performed as negative control. As expected, a strong band of the HuR protein alone was detected in the sample with no compound (positive control). Out of the thirteen compounds that we tested, three compounds, Y044-6405, STK217448, and STK018404, decreased the binding of HuR to its target RNA-motif (Figure 4A). In a second experiment testing different doses of these three compounds, only STK018404 showed a robust, dose-dependent effect on the binding of HuR to its target RNA-motif (Figure 4B).

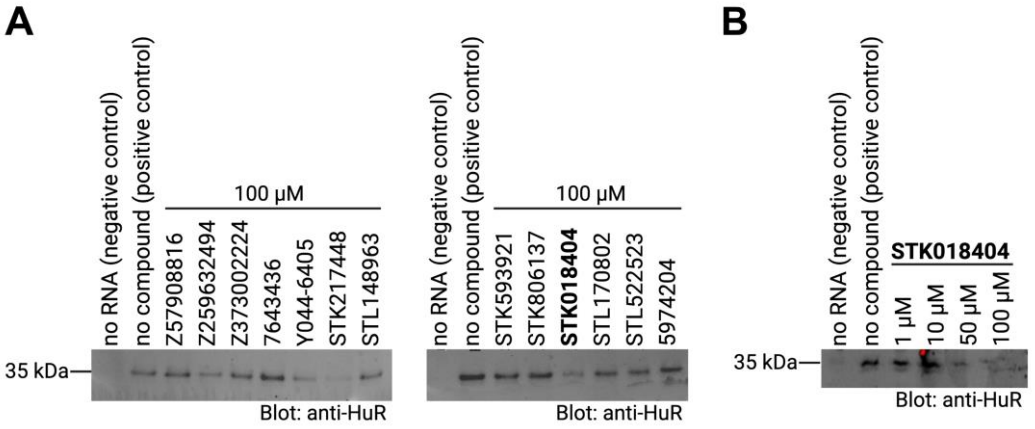

Figure 4. (**A**) RNA–protein pull-down of HuR with its target RNA motif (AUUUUUAUUUU) in the absence (positive control) or presence of the respective compounds (final concentration 100µM). RNA-bound proteins were analyzed on western blots detecting HuR. A negative control that does contain RNA and a positive control with no compound were included. (**B**) RNA–protein pull-down of HuR as described in (**A**) with different concentrations of the compound STK018404.

2.4. Docking and Fingerprints

The most promising compound according to the in vitro experiments is the representative of cluster 11, STK018404 (Figure 2B).When compared to previously reported HuR inhibitors, this small molecule is composed of novel chemotypes, namely barbituric acid and benzoic acid fused via a diazo bridge.

Our docking calculations predict that it binds to a part of the binding cleft near the linker (Figure 5A,B). It interacts with Arg97 via two hydrogen bonds and with Lys92 via a salt bridge and a hydrogen bond (Figure 5C). When compared to the PLIF of the other 12 compounds tested experimentally here, Arg97 is also identified as the most contacted residue, especially via hydrogen bonds (Figure 5D). Five residues (Ile23, Phe65, Ile103, Lys104 and Ile133) show hydrophobic interactions only, with Phe65 also displaying pi-pi-stacking interactions. Other hydrogen bonded residues are Arg153, Lys92 and Tyr63. π-cation interactions are only seen for Arg97 and a small number of salt bridges for Arg97 and Arg153. Out of the nine residues predicted to form interactions with STK018404, four have been shown by NMR to interact with other HuR inhibitors (Arg97, Ile103, Ile133 and Arg153) [24,50,56], whereas three other (Phe65, Lys92 and Lys104) are known to participate in RNA binding by X-ray crystallography [45].

Preprints (www.preprints.org) | NOT PEER-REVIEWED | Posted: 3 August 2023 doi:10.20944/preprints202308.0290.v1

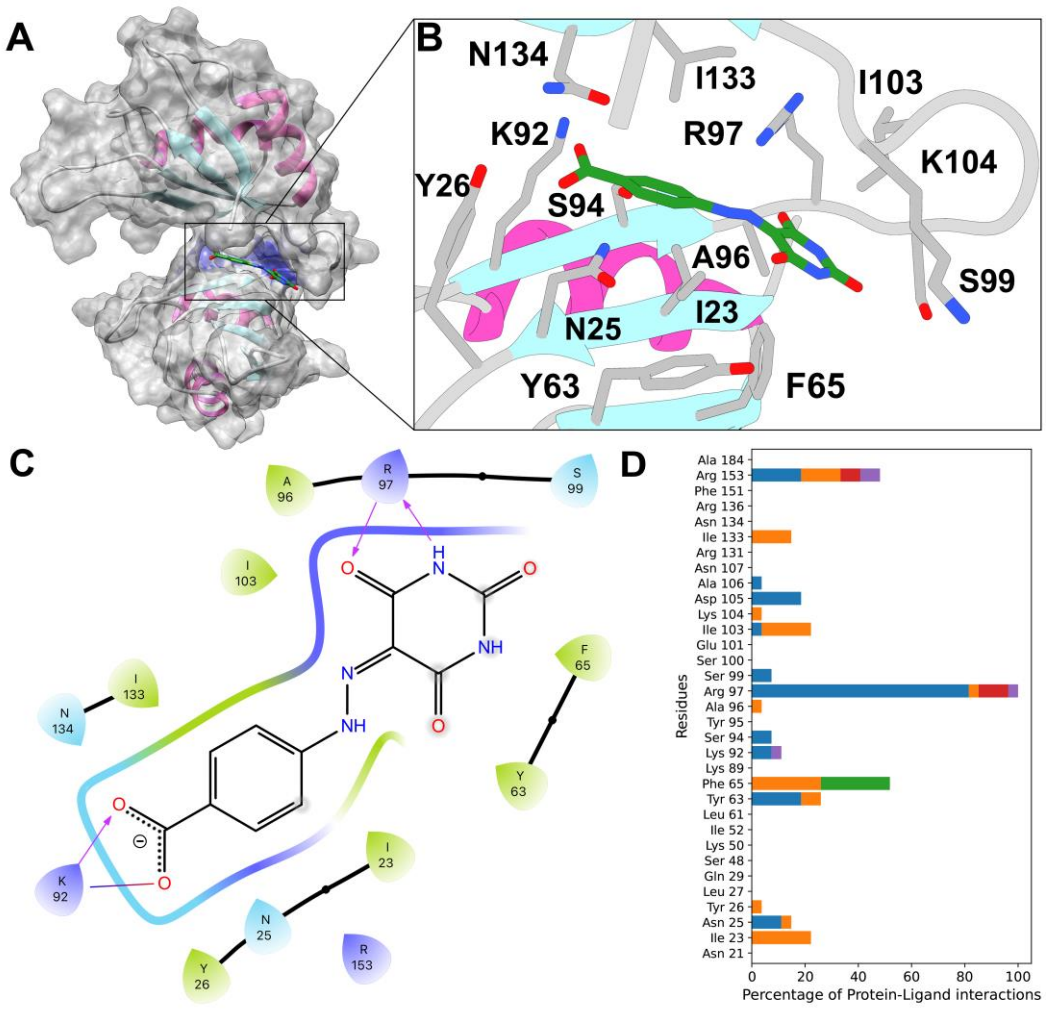

Figure 5. (**A**) Compound STK018404 in the HuR RRM1/2 transient binding cleft, with the protein surface in gray and Lys 92 (left) and Arg 97 (right) colored in purple. (**B**) Docking pose in licorice fashion of compound STK018404 (green carbons) with labeled residues (gray carbons) within 4 Å of the ligands. The protein backbone is displayed as cartoon representation, with α-helices in magenta, β-sheets in cyan and coils in gray. (**C**) Corresponding PLIF as 2D interaction diagram (with hydrogen bonds in purple and salt bridge as line turning from blue to red). The color of the residues indicates hydrophobicity (green), positive charge (violet) and polarity (cyan), whereas the light gray spheres on the ligand denote solvent exposure. The colorful thick line surrounding the ligand represents the binding cavity, with the color property being the same as for the interacting residues. Gaps in this line indicate solvent exposure of the ligand. Black lines connecting consecutive residues represent the protein backbone. (**D**) PLIF of the other tested molecules as bar plot (blue: hydrogen bonds, purple: salt bridges, orange: hydrophobic interactions, green: π-π-stacking, red: π-cation interaction). For the sake of completeness the PLIF of each of the twelve compounds is shown in Figure S6.

While eleven of the compounds tested experimentally here interact mainly with the linker (residues 96-103 in Figure S5), the remaining two compounds, STK018404 and STL170802 (representing clusters 11 and 7) extend further into the RNA binding cleft (Figure S6). The rigid scaffold and carboxylate moiety present in both these molecules (CR11 and CR7 in Figure 2B, respectively) allow the simultaneous formation of hydrogen bonds with the backbone of Arg97 and contacts with Lys92 (via a hydrogen bond and a salt bridge). However, STL170802 has an additional hydrophobic toluene ring that, according to our docking model, is mostly exposed to the solvent. This might be responsible for a less stable binding pose and, as a result, the reduced inhibitory effect in HuR binding of RNA.

 doi:10.20944/preprints202308.0290.v1

3. Discussion

RNA-binding proteins (RBPs) are a protein class that historically have not been extensively targeted using small molecule approaches [22]. In the past few years, however, several successful examples of small-molecules targeting RBP have highlighted their potential for therapeutic applications in various diseases [22].

HuR is a master post-transcriptional regulator that is mainly involved in messenger RNA (mRNA) translation and turnover [1]. Therefore, HuR is a potential therapeutic target of wide impact for several diseases, including cancer, inflammation, cardiovascular, muscle, kidney, and liver diseases [57]. Several small molecules have been identified, including MS-444 [40] currently in clinical trials.

Here, the application of virtual screening approaches gave access to an enlarged chemical space of molecules potentially targeting HuR and impairing RNA binding. Among the selected molecules, experimental validation identified ligand STK018404 as a promising HuR inhibitor, with a dose-dependent impairment of RNA binding. Our docking calculations predicted that it binds to the transient binding cleft (Figure 5B), which also accommodates cognate mRNA nucleobases and other small ligands [24]. STK018404 forms two hydrogen bonds with Arg97 and a hydrogen bond and a salt bridge with Lys92 (Figure 5C). These two residues are also known to interact with a variety of other ligands, including CMLD-2, Hyperoside, Rutin, Isovitexin, Novobiocin, Chlorogenic acid, 7-hydroxymatairesinol, Colchicoside [24,56] and Azaphilone-9 [50], as well as uracil nucleotides of the RNA (U8 and U9 in PDB 4ED5) [45]. However, its scaffold (Figure 5B) differs largely from those of the ligands so far identified (Figure S1 and Table S1), providing new endeavors for future drug design campaigns. In this respect, our approach was able to rationalize and highlight the common binding features across HuR inhibitors, and their shared key molecular anchoring points on HuR, independently of their chemical scaffolds. In vivo assays could assess if STK018404 encounters issues of specificity and potency, as it is the case for several other small molecules targeting HuR [29,32,33,35–37,40].

4. Materials and Methods

4.1. Experimental Methods: RNA pull-down

A biotinylated RNA-oligo comprising the HuR-binding motif (biotin-TEG-5'AUUUUUAUUUU-3' from IDT Integrated DNA Technologies) was dissolved in RNA structure buffer (10 mM Tris pH 7, 10 mM MgCl2, 100 mM KCl) at a final concentration of 100 pmol/µl = 100 µM, incubated for 10 min at 72°C, and cooled down slowly to RT. To coat Streptavidin-Agarose Beads (Sigma) with the RNA, 300 pmol RNA-oligo were added to 60 µl beads in 300 µl Buffer D (20mM Tris pH 7.9, 20% glycerol, 0,1 M KCl, 0,2 mM EDTA, 0,5 mM DTT) and incubated for 30 min at RT.

4 x 106 HEK293 T cells were seeded in a 150cm2 flask (cell bind surface), cultured for 48 hours, and harvested using a cell scraper. The cells were lysed in 1 ml Buffer D containing RNAse inhibitor (RiboLock) using sonication. Cell debris was removed by centrifugation for 10 min at 12000 x g at 4°C. After pre-clearing, the protein lysate was incubated with the RNA-coated beads at 4°C overnight in the presence or absence of the compounds. After extensive washing, RNA-bound proteins were eluted by boiling the beads in 30 µl 3x Lämmli buffer (150 mM Tris-Cl pH 6.8, 6% SDS , 30% glycerol, 15% ß-mercaptoethanol, 0.3 % bromophenol blue), for 5 min at 95°C. RNA-bound proteins were then analyzed on western blots using anti-HuR antibodies (Santa Cruz, SC5261) to detect HuR.

4.2. Computational Methods

The HuR protein structure (PDB code 4ED5) was preprocessed using the Protein Preparation Wizard from the Maestro Schrödinger Suite version 2022-1 with default parameters [58]. The protonation states of each side chain were generated using Epik for pH = 7 ± 2 [59]. Protein minimization was performed using the OPLS3 force field [60]. All water molecules were removed. Virtual screening studies were then performed with the HTVS [51,52] feature in Maestro, using a

repurposing library including all the commercialized and under development drugs retrieved from the Molport (8,084,644 molecules), Enamine (200,057) and KIT (11,046) libraries. The ligands were docked using a receptor grid, encompassing the RNA binding cleft of the HuR RRM1/2-RNA complex, as done in previous studies [23,24,36,56]. Twenty poses were generated for each ligand. The employed docking scoring function was Glidescore, an empirical function able to reproduce trends in ligand binding affinity to the same protein target, and defined by the following equation:

$$GScore = a \times vdW + b \times Coul + Lipo + Hbond + Metal + Rewards + RotB + Site \quad (1)$$

where: vdW = van der Waals interaction energy; Coul = Coulomb interaction energy; Lipo = Lipophilic-contact plus phobic-attractive term; HBond = Hydrogen-bonding term; Metal = Metal-binding term; Rewards = Various reward or penalty terms; RotB = Penalty for freezing rotatable bonds; Site = Polar interactions in the active site, and the coefficients of the vdW and Coul terms are: a = 0.050, b = 0.150 for Glide 5.0. The contribution from the Coulomb term is capped at −4 kcal/mol. The HTVS-based screening resulted in 1,221 hits (Figure 2A). Afterwards, Lipinski and reactive group filtering was performed in Maestro Schrödinger. This allowed to remove compounds with undesirable properties and to focus on drug-like hits, leaving 639 compounds. These were subsequently clustered according to the Butina clustering algorithm [53] in RDKit [61], with Daylight fingerprints and Tanimoto similarity scores [54], using a 0.3 cutoff. We then selected the 20 most populated clusters (Figure S2) and identified a representative molecule for each of them (Figure S3).

The docking poses of the molecules belonging to the 20 most populated clusters were furthermore used to determine protein-ligand-interaction-fingerprints (PLIFs) using the protein-ligand interaction profiler (PLIP) tool [62] to get insight into key binding residues (Figure S4). PLIP uses knowledge-based thresholds and geometric criteria to search for the most relevant contacts in the neighborhood of every residue and reports the interaction types [62].

Supplementary Materials: The following supporting information can be downloaded at the website of this paper posted on Preprints.org.

Author Contributions: Conceptualization, GR, MAP, AG, PC and SK.; methodology, all; software, BPJ, VW; validation, all; formal analysis, BPJ, VW, LK; investigation, all; resources, GR, MAP, AG, PC and SK; data curation, BPJ, VW, LK; writing—original draft preparation, BPJ, VW, GR, PC and MAP; writing—review and editing, all; visualization, BPJ, VW, LK.; supervision, GR, MAP, AG, PC and SK; project administration, GR, MAP, AG, PC and SK; funding acquisition, GR, MAP, AG, PC and SK. All authors have read and agreed to the published version of the manuscript.

Funding: This research was funded by German Federal Ministry of Education and Research (BMBF), grant number 01DP19004, project "Molecular simulation-based rational design of Painkillers Targeting the Opioid Receptor" (PaTOR). Open-access publication was funded by the Deutsche Forschungsgemeinschaft (DFG, German Research Foundation)-491111487. We thank the Central Library of Forschungszentrum Jülich for making the open access publication possible.

Institutional Review Board Statement: Not applicable.

Informed Consent Statement: Not applicable

Data Availability Statement: The data presented in this study are available upon request from the corresponding author.

Conflicts of Interest: The authors declare no conflict of interest.

References

1. Glisovic, T.; Bachorik, J. L.; Yong, J.; Dreyfuss, G. RNA-Binding Proteins and Post-Transcriptional Gene Regulation. FEBS Lett. 2008, 582 (14), 1977–1986. https://doi.org/10.1016/j.febslet.2008.03.004.
2. Rajasingh, J. The Many Facets of RNA-Binding Protein HuR. Trends Cardiovasc. Med. 2015, 25 (8), 684–686. https://doi.org/10.1016/j.tcm.2015.03.013.
3. Bevilacqua, A.; Ceriani, M. C.; Capaccioli, S.; Nicolin, A. Post-Transcriptional Regulation of Gene Expression by Degradation of Messenger RNAs. J. Cell. Physiol. 2003, 195 (3), 356–372. https://doi.org/10.1002/jcp.10272.

4. Xiao, H.; Ye, X.; Vishwakarma, V.; Preet, R.; Dixon, D. A. CRC-Derived Exosomes Containing the RNA Binding Protein HuR Promote Lung Cell Proliferation by Stabilizing c-Myc MRNA. Cancer Biol. Ther. 2022, 23 (1), 139–149. https://doi.org/10.1080/15384047.2022.2034455.
5. de la Peña, J. B.; Campbell, Z. T. RNA-Binding Proteins as Targets for Pain Therapeutics. Transl. Regul. Pain 2018, 4, 2–7. https://doi.org/10.1016/j.ynpai.2018.01.003.
6. Kunder, N.; de la Peña, J. B.; Lou, T.-F.; Chase, R.; Suresh, P.; Lawson, J.; Shukla, T.; Black, B. J.; Campbell, Z. T. The RNA-Binding Protein HuR Is Integral to the Function of Nociceptors in Mice and Humans. J. Neurosci. 2022, JN-RM-1630-22. https://doi.org/10.1523/JNEUROSCI.1630-22.2022.
7. Dixon, D. A.; Tolley, N. D.; King, P. H.; Nabors, L. B.; McIntyre, T. M.; Zimmerman, G. A.; Prescott, S. M. Altered Expression of the MRNA Stability Factor HuR Promotes Cyclooxygenase-2 Expression in Colon Cancer Cells. J. Clin. Invest. 2001, 108 (11), 1657–1665. https://doi.org/10.1172/JCI12973.
8. Cen, Y.; Chen, L.; Liu, Z.; Lin, Q.; Fang, X.; Yao, H.; Gong, C. Novel Roles of RNA-Binding Proteins in Drug Resistance of Breast Cancer: From Molecular Biology to Targeting Therapeutics. Cell Death Discov. 2023, 9 (1), 52. https://doi.org/10.1038/s41420-023-01352-x.
9. Hostetter, C.; Licata, L. A.; Costantino, C. L.; Witkiewicz, A.; Yeo, C.; Brody, J. R.; Keen, J. C. Cytoplasmic Accumulation of the RNA Binding Protein HuR Is Central to Tamoxifen Resistance in Estrogen Receptor Positive Breast Cancer Cells. Cancer Biol. Ther. 2008, 7 (9), 1496–1506. https://doi.org/10.4161/cbt.7.9.6490.
10. Wu, X.; Gardashova, G.; Lan, L.; Han, S.; Zhong, C.; Marquez, R. T.; Wei, L.; Wood, S.; Roy, S.; Gowthaman, R.; Karanicolas, J.; Gao, F. P.; Dixon, D. A.; Welch, D. R.; Li, L.; Ji, M.; Aubé, J.; Xu, L. Targeting the Interaction between RNA-Binding Protein HuR and FOXQ1 Suppresses Breast Cancer Invasion and Metastasis. Commun. Biol. 2020, 3 (1), 193. https://doi.org/10.1038/s42003-020-0933-1.
11. Abdelmohsen, K.; Gorospe, M. Posttranscriptional Regulation of Cancer Traits by HuR. Wiley Interdiscip. Rev. RNA 2010, 1 (2), 214–229. https://doi.org/10.1002/wrna.4.
12. Antic, D.; Lu, N.; Keene, J. D. ELAV Tumor Antigen, Hel-N1, Increases Translation of Neurofilament M MRNA and Induces Formation of Neurites in Human Teratocarcinoma Cells. Genes Dev. 1999, 13 (4), 449–461. https://doi.org/10.1101/gad.13.4.449.
13. Borgonetti, V.; Coppi, E.; Galeotti, N. Targeting the RNA-Binding Protein HuR as Potential Thera-Peutic Approach for Neurological Disorders: Focus on Amyo-Trophic Lateral Sclerosis (ALS), Spinal Muscle Atrophy (SMA) and Multiple Sclerosis. Int. J. Mol. Sci. 2021, 22 (19), 10394. https://doi.org/10.3390/ijms221910394.
14. Haeussler, J.; Haeusler, J.; Striebel, A. M.; Assum, G.; Vogel, W.; Furneaux, H.; Krone, W. Tumor Antigen HuR Binds Specifically to One of Five Protein-Binding Segments in the 3′-Untranslated Region of the Neurofibromin Messenger RNA. Biochem. Biophys. Res. Commun. 2000, 267 (3), 726–732. https://doi.org/10.1006/bbrc.1999.2019.
15. Lu, L.; Zheng, L.; Viera, L.; Suswam, E.; Li, Y.; Li, X.; Estévez, A. G.; King, P. H. Mutant Cu/Zn-Superoxide Dismutase Associated with Amyotrophic Lateral Sclerosis Destabilizes Vascular Endothelial Growth Factor MRNA and Downregulates Its Expression. J. Neurosci. 2007, 27 (30), 7929–7938. https://doi.org/10.1523/JNEUROSCI.1877-07.2007.
16. Li, X.; Lu, L.; Bush, D. J.; Zhang, X.; Zheng, L.; Suswam, E. A.; King, P. H. Mutant Copper-Zinc Superoxide Dismutase Associated with Amyotrophic Lateral Sclerosis Binds to Adenine/Uridine-Rich Stability Elements in the Vascular Endothelial Growth Factor 3′-Untranslated Region. J. Neurochem. 2009, 108 (4), 1032–1044. https://doi.org/10.1111/j.1471-4159.2008.05856.x.
17. Zhou, H.; Jarujaron, S.; Gurley, E. C.; Chen, L.; Ding, H.; Studer, E.; Pandak, W. M.; Hu, W.; Zou, T.; Wang, J.-Y.; Hylemon, P. B. HIV Protease Inhibitors Increase TNF-α and IL-6 Expression in Macrophages: Involvement of the RNA-Binding Protein HuR. Atherosclerosis 2007, 195 (1), e134–e143. https://doi.org/10.1016/j.atherosclerosis.2007.04.008.
18. Sengupta, S.; Jang, B.-C.; Wu, M.-T.; Paik, J.-H.; Furneaux, H.; Hla, T. The RNA-Binding Protein HuR Regulates the Expression of Cyclooxygenase-2 *. J. Biol. Chem. 2003, 278 (27), 25227–25233. https://doi.org/10.1074/jbc.M301813200.
19. Cok, S. J.; Acton, S. J.; Morrison, A. R. The Proximal Region of the 3′-Untranslated Region of Cyclooxygenase-2 Is Recognized by a Multimeric Protein Complex Containing HuR, TIA-1, TIAR, and the Heterogeneous Nuclear Ribonucleoprotein U *. J. Biol. Chem. 2003, 278 (38), 36157–36162. https://doi.org/10.1074/jbc.M302547200.

20. Lal, P.; Cerofolini, L.; D'Agostino, V. G.; Zucal, C.; Fuccio, C.; Bonomo, I.; Dassi, E.; Giuntini, S.; Di Maio, D.; Vishwakarma, V.; Preet, R.; Williams, S. N.; Fairlamb, M. S.; Munk, R.; Lehrmann, E.; Abdelmohsen, K.; Elezgarai, S. R.; Luchinat, C.; Novellino, E.; Quattrone, A.; Biasini, E.; Manzoni, L.; Gorospe, M.; Dixon, D. A.; Seneci, P.; Marinelli, L.; Fragai, M.; Provenzani, A. Regulation of HuR Structure and Function by Dihydrotanshinone-I. Nucleic Acids Res. 2017, 45 (16), 9514–9527. https://doi.org/10.1093/nar/gkx623.
21. Della Volpe, S.; Nasti, R.; Queirolo, M.; Unver, M. Y.; Jumde, V. K.; Dömling, A.; Vasile, F.; Potenza, D.; Ambrosio, F. A.; Costa, G.; Alcaro, S.; Zucal, C.; Provenzani, A.; Di Giacomo, M.; Rossi, D.; Hirsch, A. K. H.; Collina, S. Novel Compounds Targeting the RNA-Binding Protein HuR. Structure-Based Design, Synthesis, and Interaction Studies. ACS Med. Chem. Lett. 2019, 10 (4), 615–620. https://doi.org/10.1021/acsmedchemlett.8b00600.
22. Wu, P. Inhibition of RNA-Binding Proteins with Small Molecules. Nat. Rev. Chem. 2020, 4 (9), 441–458. https://doi.org/10.1038/s41570-020-0201-4.
23. Manzoni, L.; Zucal, C.; Maio, D. D.; D'Agostino, V. G.; Thongon, N.; Bonomo, I.; Lal, P.; Miceli, M.; Baj, V.; Brambilla, M.; Cerofolini, L.; Elezgarai, S.; Biasini, E.; Luchinat, C.; Novellino, E.; Fragai, M.; Marinelli, L.; Provenzani, A.; Seneci, P. Interfering with HuR–RNA Interaction: Design, Synthesis and Biological Characterization of Tanshinone Mimics as Novel, Effective HuR Inhibitors. J. Med. Chem. 2018, 61 (4), 1483–1498. https://doi.org/10.1021/acs.jmedchem.7b01176.
24. Nasti, R.; Rossi, D.; Amadio, M.; Pascale, A.; Unver, M. Y.; Hirsch, A. K. H.; Collina, S. Compounds Interfering with Embryonic Lethal Abnormal Vision (ELAV) Protein–RNA Complexes: An Avenue for Discovering New Drugs: Miniperspective. J. Med. Chem. 2017, 60 (20), 8257–8267. https://doi.org/10.1021/acs.jmedchem.6b01871.
25. Duan, L.-J.; Wang, Q.; Zhang, C.; Yang, D.-X.; Zhang, X.-Y. Potentialities and Challenges of MRNA Vaccine in Cancer Immunotherapy. Front. Immunol. 2022, 13, 923647. https://doi.org/10.3389/fimmu.2022.923647.
26. Kwak, H.-J.; Jeong, K.-C.; Chae, M.-J.; Kim, S.-Y.; Park, W.-Y. Flavonoids Inhibit the AU-Rich Element Binding of HuC. BMB Rep. 2009, 42 (1), 41–46. https://doi.org/10.5483/BMBRep.2009.42.1.041.
27. Wu, X.; Lan, L.; Wilson, D. M.; Marquez, R. T.; Tsao, W.; Gao, P.; Roy, A.; Turner, B. A.; McDonald, P.; Tunge, J. A.; Rogers, S. A.; Dixon, D. A.; Aubé, J.; Xu, L. Identification and Validation of Novel Small Molecule Disruptors of HuR-MRNA Interaction. ACS Chem. Biol. 2015, 10 (6), 1476–1484. https://doi.org/10.1021/cb500851u.
28. Wang, Z.; Bhattacharya, A.; Ivanov, D. N. Identification of Small-Molecule Inhibitors of the HuR/RNA Interaction Using a Fluorescence Polarization Screening Assay Followed by NMR Validation. PLOS ONE 2015, 10 (9), e0138780. https://doi.org/10.1371/journal.pone.0138780.
29. Meisner, N.-C.; Hintersteiner, M.; Mueller, K.; Bauer, R.; Seifert, J.-M.; Naegeli, H.-U.; Ottl, J.; Oberer, L.; Guenat, C.; Moss, S.; Harrer, N.; Woisetschlaeger, M.; Buehler, C.; Uhl, V.; Auer, M. Identification and Mechanistic Characterization of Low-Molecular-Weight Inhibitors for HuR. Nat. Chem. Biol. 2007, 3 (8), 508–515. https://doi.org/10.1038/nchembio.2007.14.
30. Julio, A. R.; Backus, K. M. New Approaches to Target RNA Binding Proteins. Gener. Ther. 2021, 62, 13–23. https://doi.org/10.1016/j.cbpa.2020.12.006.
31. Newman, D. J.; Cragg, G. M. Natural Products as Sources of New Drugs over the Nearly Four Decades from 01/1981 to 09/2019. J. Nat. Prod. 2020, 83 (3), 770–803. https://doi.org/10.1021/acs.jnatprod.9b01285.
32. Dai, Y.; Jiao, H.; Teng, G.; Wang, W.; Zhang, R.; Wang, Y.; Hebbard, L.; George, J.; Qiao, L. Embelin Reduces Colitis-Associated Tumorigenesis through Limiting IL-6/STAT3 Signaling. Mol. Cancer Ther. 2014, 13 (5), 1206–1216. https://doi.org/10.1158/1535-7163.MCT-13-0378.
33. Sun, L.; Zhang, S.; Jiang, Z.; Huang, X.; Wang, T.; Huang, X.; Li, H.; Zhang, L. Triptolide Inhibits COX-2 Expression by Regulating MRNA Stability in TNF-α-Treated A549 Cells. Biochem. Biophys. Res. Commun. 2011, 416 (1–2), 99–105. https://doi.org/10.1016/j.bbrc.2011.11.004.
34. Mutka, S. C.; Yang, W. Q.; Dong, S. D.; Ward, S. L.; Craig, D. A.; Timmermans, P. B. M. W. M.; Murli, S. Identification of Nuclear Export Inhibitors with Potent Anticancer Activity In Vivo. Cancer Res. 2009, 69 (2), 510–517. https://doi.org/10.1158/0008-5472.CAN-08-0858.
35. Hing, Z. A.; Mantel, R.; Beckwith, K. A.; Guinn, D.; Williams, E.; Smith, L. L.; Williams, K.; Johnson, A. J.; Lehman, A. M.; Byrd, J. C.; Woyach, J. A.; Lapalombella, R. Selinexor Is Effective in Acquired Resistance to Ibrutinib and Synergizes with Ibrutinib in Chronic Lymphocytic Leukemia. Blood 2015, 125 (20), 3128–3132. https://doi.org/10.1182/blood-2015-01-621391.

36. Wu, X.; Ramesh, R.; Wang, J.; Zheng, Y.; Armaly, A. M.; Wei, L.; Xing, M.; Roy, S.; Lan, L.; Gao, F. P.; Miao, Y.; Xu, L.; Aubé, J. Small Molecules Targeting the RNA-Binding Protein HuR Inhibit Tumor Growth in Xenografts. J. Med. Chem. 2023, 66 (3), 2032–2053. https://doi.org/10.1021/acs.jmedchem.2c01723.
37. Kakuguchi, W.; Nomura, T.; Kitamura, T.; Otsuguro, S.; Matsushita, K.; Sakaitani, M.; Maenaka, K.; Tei, K. Suramin, Screened from an Approved Drug Library, Inhibits HuR Functions and Attenuates Malignant Phenotype of Oral Cancer Cells. Cancer Med. 2018, 7 (12), 6269–6280. https://doi.org/10.1002/cam4.1877.
38. D'Agostino, V. G.; Adami, V.; Provenzani, A. A Novel High Throughput Biochemical Assay to Evaluate the HuR Protein-RNA Complex Formation. PLoS ONE 2013, 8 (8), e72426. https://doi.org/10.1371/journal.pone.0072426.
39. D'Agostino, V. G.; Lal, P.; Mantelli, B.; Tiedje, C.; Zucal, C.; Thongon, N.; Gaestel, M.; Latorre, E.; Marinelli, L.; Seneci, P.; Amadio, M.; Provenzani, A. Dihydrotanshinone-I Interferes with the RNA-Binding Activity of HuR Affecting Its Post-Transcriptional Function. Sci. Rep. 2015, 5 (1), 16478. https://doi.org/10.1038/srep16478.
40. Blanco, F. F.; Preet, R.; Aguado, A.; Vishwakarma, V.; Stevens, L. E.; Vyas, A.; Padhye, S.; Xu, L.; Weir, S. J.; Anant, S.; Meisner-Kober, N.; Brody, J. R.; Dixon, D. A. Impact of HuR Inhibition by the Small Molecule MS-444 on Colorectal Cancer Cell Tumorigenesis. Oncotarget 2016, 7 (45), 74043–74058. https://doi.org/10.18632/oncotarget.12189.
41. Lang, M.; Berry, D.; Passecker, K.; Mesteri, I.; Bhuju, S.; Ebner, F.; Sedlyarov, V.; Evstatiev, R.; Dammann, K.; Loy, A.; Kuzyk, O.; Kovarik, P.; Khare, V.; Beibel, M.; Roma, G.; Meisner-Kober, N.; Gasche, C. HuR Small-Molecule Inhibitor Elicits Differential Effects in Adenomatosis Polyposis and Colorectal Carcinogenesis. Cancer Res. 2017, 77 (9), 2424–2438. https://doi.org/10.1158/0008-5472.CAN-15-1726.
42. Doller, A.; Huwiler, A.; Pfeilschifter, J.; Eberhardt, W. Protein Kinase C␣-Dependent Phosphorylation of the MRNA-Stabilizing Factor HuR: Implications for Posttranscriptional Regulation of Cyclooxygenase-2. Mol. Biol. Cell 2007, 18, 12.
43. Nagai, K.; Oubridge, C.; Jessen, T. H.; Li, J.; Evans, P. R. Crystal Structure of the RNA-Binding Domain of the U1 Small Nuclear Ribonucleoprotein A. Nature 1990, 348 (6301), 515–520. https://doi.org/10.1038/348515a0.
44. Fan, X. C.; Steitz, J. A. HNS, a Nuclear-Cytoplasmic Shuttling Sequence in HuR. Proc. Natl. Acad. Sci. 1998, 95 (26), 15293. https://doi.org/10.1073/pnas.95.26.15293.
45. Wang, H.; Zeng, F.; Liu, Q.; Liu, H.; Liu, Z.; Niu, L.; Teng, M.; Li, X. The Structure of the ARE-Binding Domains of Hu Antigen R (HuR) Undergoes Conformational Changes during RNA Binding. Acta Crystallogr. D Biol. Crystallogr. 2013, 69 (3), 373–380. https://doi.org/10.1107/S0907444912047828.
46. Pabis, M.; Popowicz, G. M.; Stehle, R.; Fernández-Ramos, D.; Asami, S.; Warner, L.; García-Mauriño, S. M.; Schlundt, A.; Martínez-Chantar, M. L.; Díaz-Moreno, I.; Sattler, M. HuR Biological Function Involves RRM3-Mediated Dimerization and RNA Binding by All Three RRMs. Nucleic Acids Res. 2019, 47 (2), 1011–1029. https://doi.org/10.1093/nar/gky1138.
47. Ripin, N.; Boudet, J.; Duszczyk, M. M.; Hinniger, A.; Faller, M.; Krepl, M.; Gadi, A.; Schneider, R. J.; Šponer, J.; Meisner-Kober, N. C.; Allain, F. H.-T. Molecular Basis for AU-Rich Element Recognition and Dimerization by the HuR C-Terminal RRM. Proc. Natl. Acad. Sci. 2019, 116 (8), 2935. https://doi.org/10.1073/pnas.1808696116.
48. Filippova, N.; Yang, X.; Ananthan, S.; Sorochinsky, A.; Hackney, J. R.; Gentry, Z.; Bae, S.; King, P.; Nabors, L. B. Hu Antigen R (HuR) Multimerization Contributes to Glioma Disease Progression. J. Biol. Chem. 2017, 292 (41), 16999–17010. https://doi.org/10.1074/jbc.M117.797878.
49. (Yabukarski, F.; Biel, J. T.; Pinney, M. M.; Doukov, T.; Powers, A. S.; Fraser, J. S.; Herschlag, D. Assessment of Enzyme Active Site Positioning and Tests of Catalytic Mechanisms through X-Ray–Derived Conformational Ensembles. Proc. Natl. Acad. Sci. 2020, 117 (52), 33204–33215. https://doi.org/10.1073/pnas.2011350117.
50. Kaur, K.; Wu, X.; Fields, J. K.; Johnson, D. K.; Lan, L.; Pratt, M.; Somoza, A. D.; Wang, C. C. C.; Karanicolas, J.; Oakley, B. R.; Xu, L.; De Guzman, R. N. The Fungal Natural Product Azaphilone-9 Binds to HuR and Inhibits HuR-RNA Interaction in Vitro. PLOS ONE 2017, 12 (4), e0175471. https://doi.org/10.1371/journal.pone.0175471.
51. Friesner, R. A.; Banks, J. L.; Murphy, R. B.; Halgren, T. A.; Klicic, J. J.; Mainz, D. T.; Repasky, M. P.; Knoll, E. H.; Shelley, M.; Perry, J. K.; Shaw, D. E.; Francis, P.; Shenkin, P. S. Glide: A New Approach for Rapid,

Accurate Docking and Scoring. 1. Method and Assessment of Docking Accuracy. J. Med. Chem. 2004, 47 (7), 1739–1749. https://doi.org/10.1021/jm0306430.

52. Friesner, R. A.; Murphy, R. B.; Repasky, M. P.; Frye, L. L.; Greenwood, J. R.; Halgren, T. A.; Sanschagrin, P. C.; Mainz, D. T. Extra Precision Glide: Docking and Scoring Incorporating a Model of Hydrophobic Enclosure for Protein−Ligand Complexes. J. Med. Chem. 2006, 49 (21), 6177–6196. https://doi.org/10.1021/jm051256o.
53. Butina, D. Unsupervised Data Base Clustering Based on Daylight's Fingerprint and Tanimoto Similarity: A Fast and Automated Way To Cluster Small and Large Data Sets. J. Chem. Inf. Comput. Sci. 1999, 39 (4), 747–750. https://doi.org/10.1021/ci9803381.
54. Bajusz, D.; Rácz, A.; Héberger, K. Why Is Tanimoto Index an Appropriate Choice for Fingerprint-Based Similarity Calculations? J. Cheminformatics 2015, 7 (1), 20. https://doi.org/10.1186/s13321-015-0069-3.
55. McInnes, L.; Healy, J.; Melville, J. UMAP: Uniform Manifold Approximation and Projection for Dimension Reduction. arXiv September 17, 2020. http://arxiv.org/abs/1802.03426 (accessed 2023-06-21).
56. Vasile, F.; Della Volpe, S.; Ambrosio, F. A.; Costa, G.; Unver, M. Y.; Zucal, C.; Rossi, D.; Martino, E.; Provenzani, A.; Hirsch, A. K. H.; Alcaro, S.; Potenza, D.; Collina, S. Exploration of Ligand Binding Modes towards the Identification of Compounds Targeting HuR: A Combined STD-NMR and Molecular Modelling Approach. Sci. Rep. 2018, 8 (1), 13780. https://doi.org/10.1038/s41598-018-32084-z.
57. Schultz, C. W.; Preet, R.; Dhir, T.; Dixon, D. A.; Brody, J. R. Understanding and Targeting the Disease-Related RNA Binding Protein Human Antigen R (HuR). WIREs RNA 2020, 11 (3), e1581. https://doi.org/10.1002/wrna.1581.
58. Greenwood, J. R.; Calkins, D.; Sullivan, A. P.; Shelley, J. C. Towards the Comprehensive, Rapid, and Accurate Prediction of the Favorable Tautomeric States of Drug-like Molecules in Aqueous Solution. J. Comput. Aided Mol. Des. 2010, 24 (6–7), 591–604. https://doi.org/10.1007/s10822-010-9349-1.
59. Shelley, J. C.; Cholleti, A.; Frye, L. L.; Greenwood, J. R.; Timlin, M. R.; Uchimaya, M. Epik: A Software Program for PKaprediction and Protonation State Generation for Drug-like Molecules. J. Comput. Aided Mol. Des. 2007, 21 (12), 681–691. https://doi.org/10.1007/s10822-007-9133-z.
60. Harder, E.; Damm, W.; Maple, J.; Wu, C.; Reboul, M.; Xiang, J. Y.; Wang, L.; Lupyan, D.; Dahlgren, M. K.; Knight, J. L.; Kaus, J. W.; Cerutti, D. S.; Krilov, G.; Jorgensen, W. L.; Abel, R.; Friesner, R. A. OPLS3: A Force Field Providing Broad Coverage of Drug-like Small Molecules and Proteins. J. Chem. Theory Comput. 2016, 12 (1), 281–296. https://doi.org/10.1021/acs.jctc.5b00864.
61. RDKit. https://doi.org/10.5281/zenodo.8053810.
62. Salentin, S.; Schreiber, S.; Haupt, V. J.; Adasme, M. F.; Schroeder, M. PLIP: Fully Automated Protein–Ligand Interaction Profiler. Nucleic Acids Res. 2015, 43 (W1), W443–W447. https://doi.org/10.1093/nar/gkv315.
63. Cheng, Y.-C.; Liou, J.-P.; Kuo, C.-C.; Lai, W.-Y.; Shih, K.-H.; Chang, C.-Y.; Pan, W.-Y.; Tseng, J. T.; Chang, J.-Y. MPT0B098, a Novel Microtubule Inhibitor That Destabilizes the Hypoxia-Inducible Factor-1α MRNA through Decreasing Nuclear–Cytoplasmic Translocation of RNA-Binding Protein HuR. Mol. Cancer Ther. 2013, 12 (7), 1202–1212. https://doi.org/10.1158/1535-7163.MCT-12-0778.
64. Lee, J.-Y.; Chung, T.-W.; Choi, H.-J.; Lee, C. H.; Eun, J. S.; Han, Y. T.; Choi, J.-Y.; Kim, S.-Y.; Han, C.-W.; Jeong, H.-S.; Ha, K.-T. A Novel Cantharidin Analog N-Benzylcantharidinamide Reduces the Expression of MMP-9 and Invasive Potentials of Hep3B via Inhibiting Cytosolic Translocation of HuR. Biochem. Biophys. Res. Commun. 2014, 447 (2), 371–377. https://doi.org/10.1016/j.bbrc.2014.04.035.
65. Doller, A.; Badawi, A.; Schmid, T.; Brauß, T.; Pleli, T.; Zu Heringdorf, D. M.; Piiper, A.; Pfeilschifter, J.; Eberhardt, W. The Cytoskeletal Inhibitors Latrunculin A and Blebbistatin Exert Antitumorigenic Properties in Human Hepatocellular Carcinoma Cells by Interfering with Intracellular HuR Trafficking. Exp. Cell Res. 2015, 330 (1), 66–80. https://doi.org/10.1016/j.yexcr.2014.09.010.
66. Chae, M.-J.; Sung, H. Y.; Kim, E.-H.; Lee, M.; Kwak, H.; Chae, C. H.; Kim, S.; Park, W.-Y. Chemical Inhibitors Destabilize HuR Binding to the AU-Rich Element of TNF-α MRNA. Exp. Mol. Med. 2009, 41 (11), 824. https://doi.org/10.3858/emm.2009.41.11.088.